Influence of Amino Acid Substitutions Related to Inherited Human Prion Diseases on the Thermodynamic Stability of the Cellular Prion Protein†

Susanne Liemann*,‡ and Rudi Glockshuber

Institut für Molekularbiologie und Biophysik, Eidgenössische Technische Hochschule Hönggerberg, CH-8093 Zürich, Switzerland

Received November 13, 1998; Revised Manuscript Received January 15, 1999

ABSTRACT: Transmissible spongiform encephalopathies (TSEs) are caused by a unique infectious agent which appears to be identical with PrP^{Sc}, an oligomeric, misfolded isoform of the cellular prion protein, PrP^{C}. All inherited forms of human TSEs, i.e., familial Creutzfeldt−Jakob disease, Gerstmann−Sträussler−Scheinker syndrome, and fatal familial insomnia, segregate with specific point mutations or insertions in the gene coding for human PrP. Here we have tested the hypothesis that these mutations destabilize PrP^{C} and thus facilitate its conversion into PrP^{Sc}. Eight of the disease-specific amino acid replacements are located in the C-terminal domain of PrP^{C}, PrP(121−231), which constitutes the only part of PrP^{C} with a defined tertiary structure. Introduction of all these replacements into PrP(121−231) yielded variants with the same spectroscopic characteristics as wild-type PrP(121−231) and similar to full-length PrP(23−231), which excludes the possibility that the exchanges a priori induce a PrP^{Sc}-like conformation. The thermodynamic stabilities of the variants do not correlate with specific disease phenotypes. Five of the amino acid replacements destabilize PrP(121−231), but the other variants have the same stability as the wild-type protein. These data suggest that destabilization of PrP^{C} is neither a general mechanism underlying the formation of PrP^{Sc} nor the basis of disease phenotypes in inherited human TSEs.

Transmissible spongiform encephalopathies (TSEs)[1] or prion diseases are manifest as sporadic, infectious, or genetic disorders that are characterized by the accumulation of an abnormal isoform (PrP^{Sc}) of the cellular prion protein (PrP^{C}) in the brain (*1*, *2*). TSEs are fatal neurodegenerative diseases with long incubation periods and include scrapie in sheep and goats and bovine spongiform encephalopathy (BSE) in cattle as well as Creutzfeldt−Jakob disease (CJD), Gerstmann−Sträussler−Scheinker syndrome (GSS), fatal familial insomnia (FFI), and kuru in man. The "protein-only" hypothesis states that the infectious agent of TSEs is devoid of informational nucleic acid and is composed largely, if not entirely, of PrP^{Sc} (*3*−*5*). Since PrP^{C} and PrP^{Sc} are encoded by a single chromosomal host gene (*6*) and no differences between the covalent structures of both isoforms have yet been observed (*7*), PrP^{Sc} appears to be derived from PrP^{C} by a posttranslational mechanism in which PrP^{Sc} imposes a profound conformational change on PrP^{C} (*5*, *8*). There is numerous evidence that PrP^{C} and PrP^{Sc} indeed have different three-dimensional structures. PrP^{C} is monomeric, soluble in detergents, sensitive to proteases, and has a high α-helical content (*9*−*11*), while PrP^{Sc} is an insoluble oligomeric amyloid with a high *β*-sheet content (*9*, *12*, *13*) and is partially protease-resistant (*14*−*16*). Although there are still considerable uncertainties about the nature of the infectious TSE agent (*17*), there is compelling evidence that the generation of TSEs is dependent on PrP^{C}, as mice devoid of PrP are resistant to scrapie (*18*) and reintroduction of the PrP gene restores susceptibility to scrapie in a dose-dependent manner (*18*, *19*).

Mammalian PrP^{C} is a highly conserved cell surface glycoprotein of 209 amino acid residues (208 residues in murine PrP^{C}) (*20*, *21*) and anchored to the cell membrane via a glycosylphosphatidylinositol (GPI) moiety at its C-terminal Ser231 (*22*, *23*). Further posttranslational modifications are two N-glycosylation sites at Asn181 and Asn197 (*24*), and a single disulfide bond between Cys179 and Cys214 (*25*). Recently, the three-dimensional structures of recombinant PrP^{C} from mouse (*11*, *26*, *27*) and hamster (*10*, *28*) have been determined by NMR spectroscopy, revealing that the C-terminal residues 121−231 form a globular domain with three α-helices and a short antiparallel *β*-sheet, while the N-termimal segment 23−231 is flexibly disordered in solution. The role of the flexible N-terminal segment is not yet understood, but experiments with transgenic mice

† This work was supported by the Schweizerische Nationalfonds (Project 438+-050285) and the ETH Zürich.

* To whom correspondence should be addressed. Telephone: +1-(617)355-6240. Fax: +1-(617)355-3506. E-mail: liemann@crystal.harvard.edu.

‡ Present address: Laboratory of Molecular Medicine, Children's Hospital, 320 Longwood Ave., Boston, MA 02115.

[1] Abbreviations: TSE, transmissible spongiform encephalopathy; CD, circular dichroism; CJD, Creutzfeldt−Jakob disease; DTT, 1,4-dithio-DL-threitol; EDTA, ethylenediaminetetraacetic acid; GPI, glycosylphosphatidylinositol; GSS, Gerstmann−Sträussler−Scheinker syndrome; HPLC, high-performance liquid chromatography; *h*PrP, human PrP; IPTG, isopropyl-*β*,D-thiogalactopyranoside; FFI, fatal familial insomnia; MALDI, matrix-assisted laser desorption ionization; MES, 2-(*N*-morpholino)ethanesulfonic acid; MOPS, 4-morpholinepropanesulfonic acid; *m*PrP, murine PrP; NMR, nuclear magnetic resonance; OD, optical density; SDS−PAGE, sodium dodecyl sulfate−polyacrylamide gel electrophoresis; Tris, tris(hydroxymethyl)aminomethane; wt, wild type.

10.1021/bi982714g CCC: $18.00
Published on Web 02/26/1999

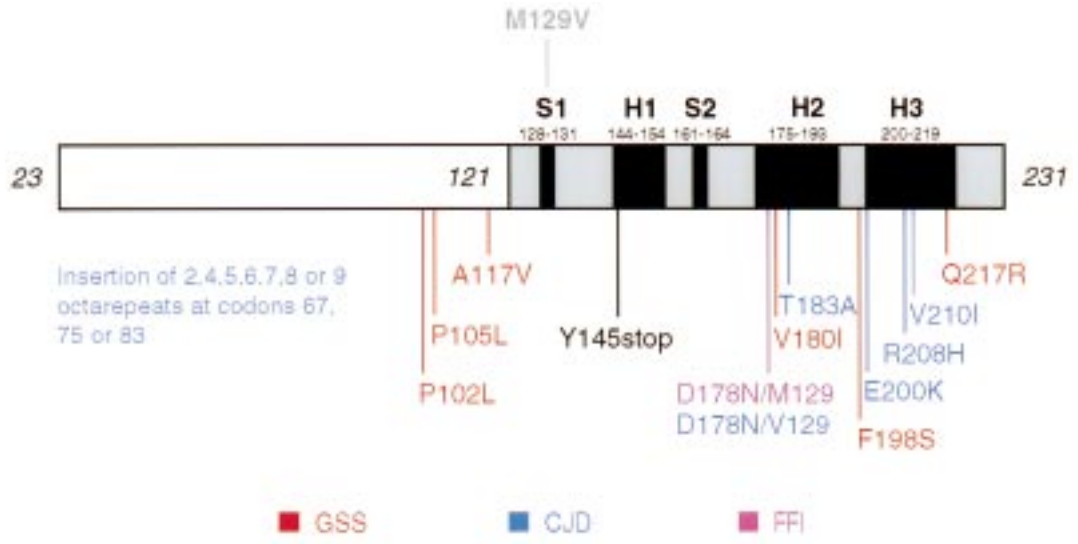

FIGURE 1: Scheme of the primary structure of mature human PrP(23−231) with the known amino acid replacements related to inherited human prion diseases indicated in different colors: CJD, blue; GSS, red; FFI, pink; human polymorphism Met129Val, gray. Residues that are replaced in inherited human TSEs are identical in the sequence of human and murine wild-type PrP. The C-terminal domain comprising residues 121−231 is shown in gray; regular secondary structure elements derived from the refined NMR structure of *m*PrP(121−231) (27) are presented by black bars.

exclusively expressing PrP lacking residues 32−121 suggest that the N-terminal tail specifically interacts with a ligand and may be required for signal transduction (*29*).

One of the strongest arguments supporting the "protein-only" hypothesis is that all known forms of inherited human TSEs, i.e., familial CJD, GSS, and FFI, are linked with dominant mutations in the gene coding for human PrP, even though not each mutation in PrP necessarily leads to spontaneous development of the disease (*30*, *31*). At present, 12 different specific point mutations and several insertions in the open reading frame of the human PrP gene have been linked with these familial TSE forms (Figure 1).

In this study we have tested the hypothesis that amino acid substitutions associated with inherited human TSEs decrease the thermodynamic stability of PrP^{C} and thus facilitate its spontaneous conversion into PrP^{Sc} (*32*−*34*). We have focused on the eight known amino acid replacements in the C-terminal domain of the prion protein, because only amino acid exchanges in the folded part of PrP^{C} are expected to have an effect on protein stability. As a model system, we used the C-terminal domain of murine PrP^{C} comprising residues 121−231 (amino acid residue numbering according to human PrP; *20*) (Figure 2). *m*PrP(121−231) shares 94% sequence identity with human PrP(121−231) and is thus expected to have a very similar three-dimensional structure. Most importantly, all eight residues in segment 121−231 of human PrP whose replacements segregate with inherited TSEs are idential in wild-type human and mouse PrP(121−231), and the side chains which are in direct contact with these residues in the NMR structure of *m*PrP(121−231) are also identical (*26*, *27*).

We have introduced all these eight amino acid exchanges separately into *m*PrP(121−231), as well as the Met129Val substitution that corresponds to the polymorphism in human PrP determining the disease phenotype linked to the Asp178Asn mutation (*35*), and the replacement Thr190Val that corresponds to a polymorphism at positions 108 and 189 in mouse PrP determining the scrapie incubation time in mice

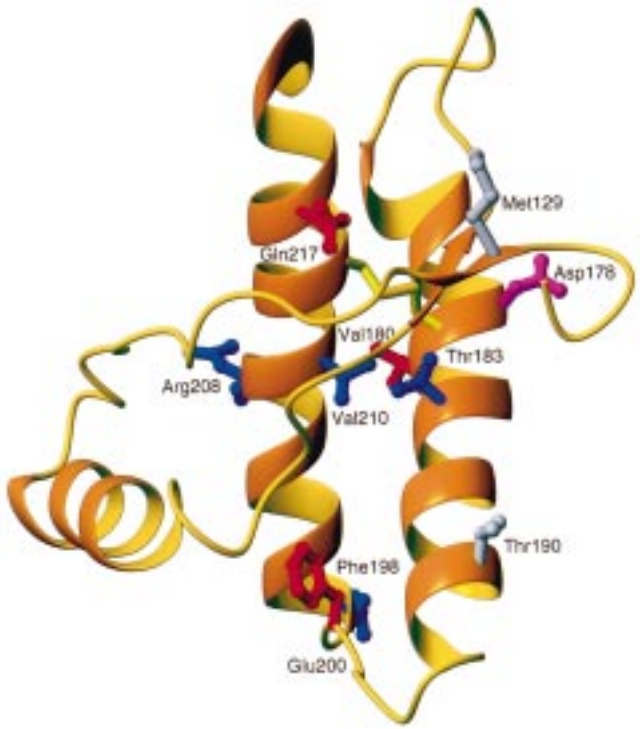

FIGURE 2: Ribbon diagram of the refined NMR structure of *m*PrP-(121−231) (27). Amino acid side chains that are replaced in inherited human TSEs are shown in the same color code as in Figure 1 (amino acid residue numbering of *m*PrP according to *h*PrP; *20*). The side chains of residues 129 and 190, corresponding to polymorphism sites in human and murine PrP, respectively, are depicted in gray. The figure was created with MOLMOL (93)

(*36*). We expressed all the variants in the periplasm of *Escherichia coli* and find that exactly those amino acid exchanges which destabilize *m*PrP(121−231) lead to formation of periplasmic inclusion bodies, while the other exchanges yielded soluble protein, as observed for wild-type *m*PrP(121−231). We present a complete study on the spectroscopic properties and thermodynamic stabilities of all these *m*PrP(121−231) variants and compare these findings

with the characteristics of recombinant full-length *m*PrP(23−231). We demonstrate that none of the amino acid exchanges is sufficient to induce a PrP^{Sc}-like conformation in *m*PrP-(121−231) and that destabilization of PrP^{C} is unlikely to be a general mechanism underlying the facilitated formation of PrP^{Sc} in inherited TSEs.

EXPERIMENTAL PROCEDURES

Plasmids and Oligonucleotides Used for Site-Directed Mutagenesis. The phagemid pPrP-CRR (*37*) was used for construction and expression of *m*PrP(121−231) mutants. Site-directed mutagenesis was performed according to (*38*, *39*) using uridinylated single-stranded pPrP-CRR from phage infection (*40*) of the *E. coli* strain CJ236 (Mutagene phagemid kit, Bio Rad). Mutants were identified by restriction analysis and verified by complete dideoxynucleotide sequencing using the Thermo Sequenase sequencing kit (Amersham). For expression of *m*PrP(23−231), the phagemid pPrP was used in which the gene coding for mature murine full-length PrP was cloned into the plasmid pRBI-PDI-T7t-Nde (Hermanns and Glockshuber, unpublished) via the *Nde*I and *Bam*HI restriction sites using the described oligonucleotide primers for amplification of the *m*PrP gene (*41*). pRBI-PDI-T7t-Nde is a derivative of pRBI-PDI-T7 (*42*) which additionally contains a T7 terminator and a single *Nde*I restriction site at the start codon. In both pPrP-CRR and pPrP, the *m*PrP gene is under control of the T7 promotor/lac operator sequence (*43*), but only in pPrP-CRR the mPRP gene is fused to the bacterial OmpA signal sequence for secretory periplasmic expression. Recombinant *m*PrP(121−231) and *m*PrP(23−231) contain an additional serine residue at both their C- and N-termini.

Purification of mPrP(121−231) Wild Type and Soluble Variants from Periplasmic Extracts. Cells of *E. coli* BL21-(DE3) harboring the respective derivative of pPrP-CRR were grown at 37 °C in 12 L of LB medium containing 100 μg/mL ampicillin. At an optical density (OD) at 550 nm of 1.5, isopropyl-β,D-thiogalactoside (IPTG) was added to a final concentration of 1 mM, and cell growth was continued for 12 h at 26 °C. The cells were harvested by centrifugation, suspended in ice-cold buffer A [50 mM Tris-HCl (pH 8.0), 150 mM NaCl, 5 mM EDTA, 1 mg/mL polymyxin-B-sulfate; 2 mL/g wet cells], stirred for 1 h at 4 °C, and centrifuged (30 min, 49000*g*, 4 °C). The supernatant was treated with 0.57 mM phenylmethylsulfonyl chloride and 0.7 μg/mL pepstatin A (final concentrations), dialyzed against 10 mM MES−NaOH (pH 5.8) [or against 10 mM sodium acetate (pH 5.0) in the case of variant Arg208His], and applied to a CM52 cellulose column (30 mL; Whatman). *m*PrP(121−231) was eluted with a linear gradient (800 mL) from 0 to 400 mM NaCl in 10 mM MES−NaOH (pH 5.8) [or 10 mM sodium acetate (pH 5.0) in the case of variant Arg208His]. *m*PrP(121−231) was further purified by hydrophobic chromatography on Phenyl-Sepharose High Performance (15 mL; Pharmacia) and gel filtration on Superdex 75 (320 mL; Pharmacia) as described (*37*). Proteins were stored at −20 °C in 50 mM sodium phosphate (pH 7.0). The molecular mass of each variant was confirmed by MALDI mass spectrometry (error ≤5 Da). The yields of the purified proteins varied between 0.5 and 7.5 mg/L of bacterial culture.

Purification of mPrP(121−231) Variants from Periplasmic Inclusion Bodies. Cells of *E. coli* BL21(DE3) harboring the respective derivative of pPrP-CRR were grown at 37 °C in 12 L of LB medium containing 100 μg/mL ampicillin. When the OD at 550 nm had reached a value of 1.5, IPTG was added to a final concentration of 1 mM, and the cells were incubated for 12 h at 33 °C. The cells were harvested by centrifugation, resuspended in ice-cold buffer B [50 mM Tris-HCl (pH 8.0), 150 mM NaCl, 5 mM EDTA; 2 mL/g wet cells], treated with 0.57 mM phenylmethylsulfonyl fluoride, 0.7 μg/mL pepstatin A (final concentrations), and disrupted in a French pressure cell (18 000 psi; SLM-Aminco). After centrifugation (30 min, 49000*g*, 4 °C), the inclusion bodies were washed twice in buffer C [20 mM Tris-HCl (pH 8.0), 100 mM NaCl, 1 mM benzamidine, 0.5 mM EDTA, 1% (v/v) Triton X-100], then suspended in 20 mM Tris-HCl (pH 8.0), 100 mM NaCl, 2 mM $MgCl_2$, 1 mg/mL lysozyme, 0.5 mg/mL DNase I, incubated at 37 °C for 30 min, and centrifuged (15 min, 49000*g*, 4 °C). The pellet was washed twice with buffer C, once with 20 mM Tris-HCl (pH 8.0), 1 mM benzamidine, 0.5 mM EDTA, and resuspended in 100 mL of 10 mM MES−NaOH (pH 5.6), 8 M urea [the urea was deionized using a Dowex Monosphere ion exchanger (Fluka)]. After centrifugation (30 min, 49000*g*, 25 °C), the supernatant was applied to a DE52/CM52 tandem column (30 mL each; Whatman), and *m*PrP(121−231) was eluted from the CM52 column with a linear gradient (800 mL) from 0 to 400 mM NaCl in 10 mM MES−NaOH (pH 5.6), 8 M urea. The eluate was concentrated and further purified by gel filtration on Superdex 75 (320 mL; Pharmacia) in 10 mM MES−NaOH (pH 6.0), 100 mM NaCl, 8 M urea. Fractions containing *m*PrP(121−231) were pooled, concentrated to 10 mg/mL, and refolded by 1:50 dilution into 50 mM sodium phosphate (pH 7.0) at 15 °C. The solution was kept at 4 °C for 12 h, and precipitates were removed by centrifugation (30 min, 49000*g*, 4 °C). The supernatant was dialyzed against 50 mM sodium phosphate (pH 7.0) and stored at 4 °C. The molecular mass of each variant was confirmed by MALDI mass spectrometry. Formation of the single disulfide bridge was proven by the lack of free thiol groups in the unfolded proteins (*44*). The yields of the purified variants were between 0.5 and 4 mg/L of bacterial culture.

Purification of mPrP(23−231) Wild Type from Cytoplasmic Inclusion Bodies. Cells of *E. coli* BL21(DE3)/pPrP were grown at 37 °C in 2 L of rich medium [20 g/L tryptone, 10 g/L yeast extract, 85 mM NaCl, 2% (v/v) glycerol, 50 mM K_2HPO_4, 10 mM $MgCl_2$, 1% (w/v) glucose] containing 100 μg/mL ampicillin until an OD at 550 nm of 1.5 was reached. After addition of IPTG to a final concentration of 1 mM, cells were grown at 37 °C for 5 h and harvested by centrifugation. Cells were suspended at 0 °C in 25 mL of 50 mM Tris-HCl (pH 8.0), 1 mM $MgCl_2$, 0.4 mg/mL DNase I, 0.4 mg/mL RNase A, 1 mg/mL lysozyme and disrupted in a French pressure cell (18 000 psi; SLM-Aminco). The inclusion bodies were sedimented by centrifugation (30 min, 49000*g*, 4 °C) and washed with 20 mM Tris-HCl (pH 8.0), 23% (w/v) sucrose, 0.5% (v/v) Triton X-100, 1 mM EDTA, 1 mM benzamidine until the supernatant after centrifugation (15 min, 49000*g*, 4 °C) was colorless. The pellet was dissolved in 10 mM Tris-HCl (pH 8.0), 50 mM DTT, 1 mM EDTA, 8 M urea deionized using a Dowex Monosphere ion exchanger (Fluka). The solution was adjusted to pH 7.0 with 100 mM HCl and centrifuged (15 min, 49000*g*, 4 °C),

and the supernatant was applied to a DE52/SP−Sepharose tandem column (30 mL each) equilibrated with 10 mM MOPS−NaOH (pH 7.0), 5 mM DTT, 1 mM EDTA, 8 M urea. *m*PrP(23−231) was eluted from the SP−Sepharose column with a linear gradient (800 mL) from 100 to 400 mM NaCl in 10 mM MOPS−NaOH (pH 7.0), 5 mM DTT, 1 mM EDTA, 8 M urea. All fractions containing *m*PrP(23−231) were combined, concentrated, and applied to a Superdex-200 column (Pharmacia; 320 mL). *m*PrP(23−231) was eluted with 10 mM MES−NaOH (pH 6.0), 100 mM NaCl, 8 M urea. The pooled fractions with *m*PrP(23−231) were diluted with 100 mM Tris-HCl (pH 8.5), 8 M urea to a protein concentration of 0.05 mg/mL. $CuSO_4$ was added to a final concentration of 1 μM, and the solution was stirred for 2 h at room temperature. Formation of the single disulfide bond was analyzed by separation of acid-quenched samples (pH <2) on an analytical reversed-phase HPLC column (Vydac C18, 4.6 × 250 mm) at 55 °C with a linear gradient from 30 to 55% (v/v) acetonitrile in 0.1% (v/v) trifluoroacetic acid (flow rate: 2 mL/min). The oxidation reaction was quenched by addition of 1 mM EDTA, and the pH of the solution was subsequently adjusted to 6.5 with 100 mM HCl. The protein was concentrated to 10 mg/mL and then diluted dropwise (1:50) into 10 mM MES−NaOH (pH 6.0), 1 mM EDTA at 15 °C. The solution was stirred for 12 h at 4 °C and applied to a CM52 column (15 mL) equilibrated with 10 mM MES−NaOH (pH 6.0), 1 mM EDTA. *m*PrP(23−231) was eluted with a linear gradient (400 mL) from 100 to 600 mM NaCl in 10 mM MES−NaOH (pH 6.0), 1 mM EDTA. Fractions containing pure *m*PrP(23−231) were combined, dialyzed against water, and stored at −20 °C. The protein was stable at room temperature in the presence of 0.01% sodium azide and the protease inhibitor cocktail 'COMPLETE' (Boehringer Mannheim) for weeks. The final yield of purified *m*PrP(23−231) was 20 mg/L of bacterial culture.

Protein Concentrations. Protein concentrations were determined by the specific absorbance of the proteins according to (*45*) with $\epsilon = 19\,890\ M^{-1}\ cm^{-1}$ for *m*PrP(121−231) and $\epsilon = 62\,280\ M^{-1}\ cm^{-1}$ for *m*PrP(23−231).

Circular Dichroism Spectra. Far- and near-UV circular dichroism (CD) spectra were measured at 25 °C on a Jasco 710 CD spectropolarimeter in 0.02- and 1-cm quartz cuvettes, respectively, accumulated 16 or 32 times and corrected for the buffer. Protein samples with 38 μM *m*PrP(121−231) or 22 μM *m*PrP(23−231) in 50 mM sodium phosphate (pH 7.0) were centrifuged (30 min, 21000*g*, 4 °C) prior to the measurements in order to remove possible aggregates. For the *m*PrP(121−231) variant Thr183Ala, a maximum protein concentration of 1.9 μM was used due to its very low solubility under native conditions.

Urea-Induced Equilibrium Transitions. For unfolding experiments, the *m*PrP(121−231) variants were diluted 1:11 with 50 mM sodium phosphate (adjusted to pH 7.0) containing different urea concentrations to a final protein concentration of 19 μM *m*PrP(121−231). Full-length *m*PrP(23−231) aggregated at concentrations ≥1 mg/mL at pH 7.0, but showed a high solubility at lower pH values. Therefore, the protein was concentrated in 5 mM sodium acetate (pH 5.0) before 1:11 dilution with 55 mM sodium phosphate (pH 7.1) containing different urea concentrations, yielding a final protein concentration of 13 μM *m*PrP(23−231) in 50 mM sodium phosphate (pH 7.0). All samples were incubated for 36 h at 25 °C. For refolding experiments, the proteins were denatured in 50 mM sodium phosphate (pH 7.0), 10 M urea for 1 h at room temperature and then diluted 1:11 to the same protein concentrations as in the unfolding experiments. The equilibrium transitions were monitored at 25 °C by recording the far-UV CD signal at 222 nm for 1 min on a Jasco 710 CD spetropolarimeter in 0.1-cm cuvettes. The averaged ellipticities were corrected for the buffer. The urea concentrations were determined by refractometry (*46*). The transitions were evaluated according to a two-state equilibrium with a six-parameter fit as described (*47*). Due to the very low solubility of the *m*PrP(121−231) variant Thr183Ala in the absence of urea, only its refolding transition was measured at a protein concentration of 3 μM, which was the lowest possible concentration for obtaining a sufficient signal/noise ratio for the measurements and a sufficient number of measurement points at lower urea concentrations. Since aggregation of Thr183Ala at this concentration occurred below 1 M urea, the data were evaluated with a five-parameter fit using constant slopes for the pretransitional base line between −300 and +300 mdeg/M [corresponding to the slope range observed for all other *m*PrP(121−231) variants]. Only small differences for ΔG°_{fold} and the cooperativity (*m*-value) were observed upon variation of the pretransitional base line slope. ΔG°_{fold} ranged from -9.83 ± 0.45 to -10.97 ± 0.53 kJ mol^{-1} and the cooperativity from 3.40 ± 0.14 to 3.57 ± 0.16 kJ mol^{-1} M^{-1}. The stability data for the variant Thr183Ala shown in Table 1 were calculated with a fixed slope of +5 mdeg/M. The uncertainty about the pretransitional base line slope is contained in the given error of ±2.1 kJ mol^{-1}.

RESULTS

mPrP(121−231) and Full-Length mPrP(23−231) Have Comparable Thermodynamic Stabilities. We first compared the thermodynamic stabilities of wild-type *m*PrP(23−231) and *m*PrP(121−231) to examine whether the isolated C-terminal domain of PrP^C is a suitable model system to study the effects of point mutations in the segment 121−231 of full-length PrP^C. The domain *m*PrP(121−231) was purified after periplasmic expression in *E. coli* essentially as described (*48*) (see also Figure 3). For production of full-length *m*PrP-(23−231) from cytoplasmic inclusion bodies, we established an improved purification protocol which yielded 20 mg of purified *m*PrP(23−231) per liter of bacterial culture, i.e., a 4-fold higher yield compared to the previously described protocol (*41*) (see Experimental Procedures for details). Overall, the following changes significantly improved the yield: use of a specifically enriched growth medium instead of LB medium, induction of the cells with IPTG at 37 °C for no longer than 5 h, improved preparation of the inclusion bodies, air oxidation of the disulfide bond for 2 h at pH 8.5 in the presence of 8 M urea catalyzed by 1 μM Cu^{2+}, and refolding of oxidized *m*PrP(23−231) at pH 6.0 by dilution instead of dialysis against distilled water. Specifically, a systematic analysis of the optimal conditions for disulfide bond formation revealed that no oxidation could be achieved under nondenaturing conditions, which is in accordance with the inaccessibility of the disulfide bond in the three-dimensional structure of *m*PrP(23−231) (*11*).

Table 1: Thermodynamic Stabilities of *m*PrP(121−231) Variants, *m*PrP(121−231) Wild Type, and Full-Length *m*PrP(23−231) Wild Type at pH 7.0 and 25 °C

*m*PrP protein	prion disease phenotype	ΔG°_{fold} (kJ mol^{-1})[a]	$\Delta\Delta G^\circ_{fold}$ (variant − wild type)[b]	cooperativity (kJ mol^{-1} M^{-1})[a]	$[urea]_{1/2}$ (M)[a]
*m*PrP(121−231) wt	−	−29.7 ± 1.0	−	4.8 ± 0.2	6.2
*m*PrP(23−231) wt	−	−25.5 ± 1.0	4.2 ± 1.9	4.1 ± 0.2	6.3
M129V	polymorphism (human)	−28.2 ± 1.0	1.4 ± 2.0	4.5 ± 0.2	6.3
D178N/M129	FFI	−22.5 ± 0.7	7.2 ± 1.7	4.7 ± 0.1	4.8
D178N/V129	CJD	−21.7 ± 0.9	8.0 ± 1.8	4.5 ± 0.2	4.9
V180I	GSS	−27.6 ± 0.8	2.1 ± 1.7	4.5 ± 0.1	6.2
T183A	CJD	−10.4 ± 2.1	19.3 ± 3.1	3.5 ± 0.5	3.0
T190V	polymorphism (mouse)	−30.3 ± 1.5	−0.7 ± 2.4	4.8 ± 0.2	6.4
F198S	GSS	−19.4 ± 0.8	10.3 ± 1.7	4.4 ± 0.2	4.5
E200K	CJD	−29.1 ± 1.5	0.6 ± 2.4	4.9 ± 0.3	5.9
R208H	CJD	−23.7 ± 1.5	6.0 ± 2.5	4.3 ± 0.3	5.6
V210I	CJD	−28.6 ± 1.6	1.1 ± 2.6	4.5 ± 0.3	6.3
Q217R	GSS	−20.8 ± 0.8	8.9 ± 1.7	4.5 ± 0.2	4.7

[a] The thermodynamic stabilities were measured by urea-induced equilibrium transitions (Figure 5). Data were evaluated according to a two-state model of folding (*47*). [b] $\Delta\Delta G^\circ_{fold}$ (variant − wild type) is the difference between the free energy of folding of *m*PrP(121−231) variants [or *m*PrP(23−231) wild type] and *m*PrP(121−231) wild type.

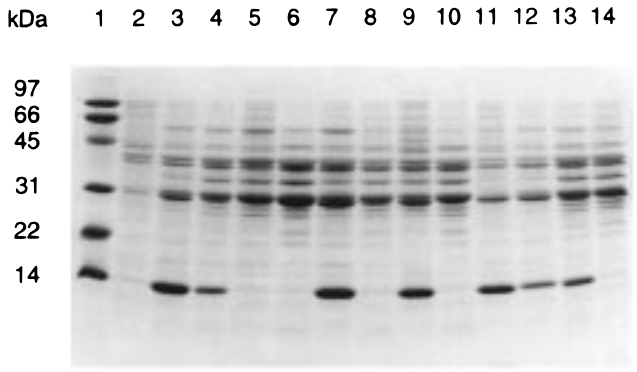

FIGURE 3: Soluble periplasmic fractions of *E. coli* BL21(DE3)/pPrP-CRR cells expressing wild type and mutant *m*PrP(121−231). A Coomassie-stained SDS−polyacrylamide gel (15% w/v) is shown. Lane 1, molecular mass standards; 2, wild-type *m*PrP(121−231) before induction with IPTG; 3, wild-type *m*PrP(121−231) 18 h after induction (same as for the variants shown in the following lanes); 4, Met129Val; 5, Met129/Asp178Asn; 6, Met129Val/Asp178Asn; 7, Val180Ile; 8, Thr183Ala; 9, Thr190Val; 10, Phe198Ser; 11, Glu200Lys; 12, Arg208His; 13, Val210Ile; 14, Gln217Arg. The exchanges Met129Val and Thr190Val correspond to natural polymorphisms in human and mouse PrP, respectively (see text). The band at approximately 14 kDa corresponds to *m*PrP-(121−231).

The thermodynamic stabilities of *m*PrP(23−231) and *m*PrP(121−231) were measured at pH 7.0 and 25 °C by urea-induced unfolding/refolding equilibria. The transitions were followed by the α-helical far-UV CD signal of the proteins at 222 nm, where *m*PrP(23−231) shows a lower mean residue ellipticity compared to *m*PrP(121−231) due to its flexibly extended N-terminal segment (*11*, *41*) (Figure 4A). *m*PrP(121−231) and *m*PrP(23−231) showed very similar, fully reversible transitions with identical midpoints at about 6.2 M urea. Analysis of the transitions according to the two-state model of folding (*47*) yielded a ΔG°_{fold} of −25.5 kJ mol^{-1} for full-length *m*PrP(23−231) compared to −29.7 kJ mol^{-1} for the isolated C-terminal domain *m*PrP(121−231) (*48*) (Figure 5, Table 1). The slightly lower stability of the full-length protein arises from a small decrease in the cooperativity of folding (*m*-value) (see Discussion). However, the transitions of the isolated C-terminal domain and the full-length protein at pH 7.0 are very similar, and we conclude that amino acid exchanges in the isolated domain *m*PrP(121−231) have the same effect on protein stability as in the full-length protein.

Some TSE-Related Variants of mPrP(121−231) Cannot Be Expressed as Soluble Protein and Form Periplasmic Inclusion Bodies. Like *m*PrP(121−231) wild type (*37*), the TSE-related variants Val180Ile, Glu200Lys, Arg208His, and Val210Ile as well the polymorphism variants Met129Val and Thr190Val were produced as soluble proteins in the periplasm of *E. coli* using the OmpA signal sequence (Figure 3) and could be purified by cation exchange chromatography, hydrophobic interaction chromatography, and gel filtration, with yields between 0.5 and 4.0 mg of pure protein/L of bacterial culture. In contrast, the variants Asp178Asn/Met129, Asp178Asn/Met129Val, Thr183Ala, Phe198Ser, and Gln217LArg could not be obtained in a soluble form in the periplasm (Figure 3). Western blot analysis of total cell extracts with polyclonal antibodies against recombinant *m*PrP(23−231) revealed that these variants accumulated in a processed, but insoluble form in periplasmic inclusion bodies. In contrast, only small quantities of insoluble protein were detected for the variants obtained as soluble protein in the periplasm (data not shown). Thus, the lack of the soluble *m*PrP(121−231) variants Asp178Asn/Met129, Asp178Asn/Met129Val, Thr183Ala, Phe198Ser, and Gln217LArg in the periplasm was due to protein aggregation and not due to proteolytic degradation of the polypeptide chains in vivo. In contrast to the cytoplasmic inclusion bodies of full-length *m*PrP(23−231), the disulfide bond was already present in the polypeptide chains aggregated in the periplasm. The periplasmic inclusion bodies were solubilized in 8 M urea, and the proteins were purified to homogeneity by cation exchange chromatography and gel filtration in the presence of 8 M urea before refolding by dilution at pH 7.0 and 15 °C. The pure *m*PrP(121−231) variants were obtained in yields of 0.5−3 mg/L of bacterial culture. The correct cleavage of the OmpA signal sequence was confirmed by mass spectrometry. All proteins could be concentrated to at least 4 mg/mL in 50 mM sodium phosphate (pH 7.0) and were well-behaved in solution, except for the variant Thr183Ala which showed a maximum solubility of 0.025 mg/mL (1.9 μM) under native conditions at pH 7.0 and extensive aggregation above this threshold.

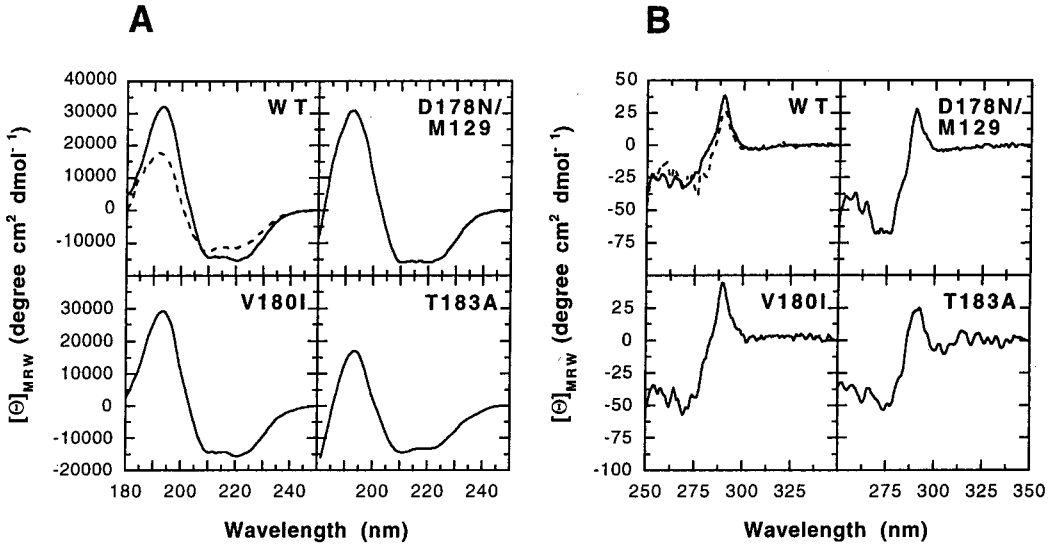

FIGURE 4: (A) Far-UV CD spectra and (B) near-UV CD spectra at pH 7.0 and 25 °C of *m*PrP(121−231) wild type (solid line), *m*PrP-(23−231) wild type (dotted line), and the *m*PrP(121−231) variants. As examples, the spectra of the variants Asp178Asn/Met129Val (associated with FFI; insoluble in the periplasm of *E. coli*), Val180Ile (GSS; soluble in the periplasm), and Thr183Ala (CJD; insoluble in the periplasm) are shown.

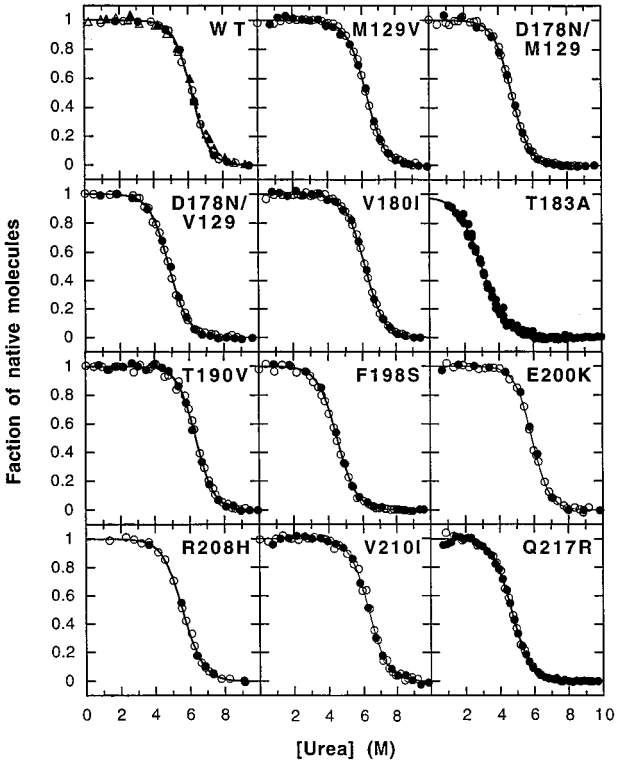

FIGURE 5: Normalized urea-induced equilibrium transitions of all *m*PrP(121−231) variants at pH 7.0 and 25 °C measured by their far-UV CD signal at 222 nm. A superposition of *m*PrP(121−231) wild type (circles; solid line) and *m*PrP(23−231) wild type (triangles; dotted line) is shown in the upper left panel with only 30% of all data points plotted. Open symbols represent unfolding, filled symbols refolding experiments. The lines correspond to fits according to the two-state model of folding (47).

All mPrP(121−231) Variants Show PrP^C-like Structural Characteristics. The influence of the amino acid replacements on the secondary and tertiary structure of *m*PrP(121−231) was analyzed by far- and near-UV CD spectroscopy, respectively. The far-UV CD spectra of all variants were practically identical to the spectrum of wild-type *m*PrP(121−231) with two minima at 208 and 222 nm, indicative for a high α-helical content (Figure 4A). No conformational changes toward an increased β-sheet content characteristic for PrP^{Sc} were apparent from the far-UV CD spectra, and no differences between the variants which were obtained as soluble or insoluble protein in the periplasm were observed. The same result was obtained for the near-UV CD spectra of the variants which all contain a characteristic maximum at about 290 nm and do not differ significantly from the near-UV CD spectrum of *m*PrP(121−231) wild type (Figure 4B). Therefore, neither the secondary nor the tertiary structure of *m*PrP(121−231) is significantly affected by any of the amino acid replacements associated with inherited human TSEs.

Several but Not All Variants of mPrP(121−231) Have Lower Thermodynamic Stabilities than the Wild-Type Protein. The thermodynamic stabilities of all variants of *m*PrP-(121−231) were determined at pH 7.0 and 25 °C by urea-induced unfolding/refolding experiments (Figure 5, Table 1). All proteins showed cooperative and fully reversible transitions. In the case of the variant Thr183Ala, which exhibits a low solubility at pH 7.0 in the absence of urea, we only could measure the refolding transition between 10 and 1 M urea (for evaluation of the data, see Experimental Procedures). Both polymorphism variants Met129Val and Thr190Val as well as the TSE-related variants Glu200Lys and Val210Ile have the same stability as *m*PrP(121−231) wild type within experimental error ($\Delta G°_{fold} \sim -29$ kJ mol^{-1}; Table 1). The amino acid exchange Val180Ile slightly destabilizes the protein by 2 kJ mol^{-1}, whereas the Arg208His replacement lowers the stability by 6 kJ mol^{-1}. In contrast to all these variants obtained in a soluble form in the periplasm of *E. coli*, all variants that accumulated as inclusion bodies show a significantly reduced intrinsic stability compared to the wild-type domain. The exchange of Asp178 by Asn destabilizes the variants Asp178Asn and Asp178Asn/Met129Val by a similar value (∼7−8 kJ mol^{-1}). Thus, residue 129 has no influence on the destabilizing effect of the Asp178Asn exchange. The amino acid substitutions Gln217Arg and Phe198Ser destabilize *m*PrP(121−231) by

10.3 and 8.9 kJ mol^{-1}, respectively, and the variant Thr183Ala shows the lowest $\Delta G°_{fold}$ of approximately 10 kJ mol^{-1} (equivalent to a destabilization of the domain by 19.3 kJ mol^{-1}). The cooperativities of the transitions of wild-type *m*PrP(121−231) and all variants are very similar with values between 4.3 and 4.9 kJ mol^{-1} M^{-1} (Table 1). Only the variant Thr183Ala exhibits a significantly reduced cooperativity of 3.5 kJ mol^{-1} M^{-1} and may thus no longer fold according to the two-state model (*49*). Overall, only some of the amino acid replacements linked with inherited TSEs destabilize *m*PrP(121−231).

DISCUSSION

Eight out of eleven amino acid substitutions associated with inherited human prion diseases are located in the C-terminal domain of the prion protein comprising residues 121−231. The replacement of these residues in recombinant *m*PrP(121−231) does not affect the global protein structure at pH 7.0 in the absence of denaturants as shown by far- and near-UV CD spectroscopy (Figure 4A,B). These data exclude the possibility that these mutations per se cause a PrP^{Sc}-like conformation and lead to soluble precursors of oligomeric PrP^{Sc}. In contrast to the hypothesis that all point mutations associated with inherited TSEs destabilize PrP^{C} (*32*−*34*), the urea-induced equilibrium transitions of all variants demonstrated either a destabilizing or no effect of the resulting amino acid replacements on protein stability (Figure 5, Table 1). Similar observations were very recently made by the investigation of three human PrP(90−231) variants (*50*). *h*PrP(90−231) Asp178Asn aggregated in inclusion bodies as its murine counterpart, and the Pro102Leu substitution within the unstructured protein tail had no influence on protein stability. In contrast to our results, the *h*PrP(90−231) Glu200Lys variant had a slightly destabilizing effect (*50*).

Furthermore, we found an excellent correlation between the thermodynamic stabilities of the *m*PrP(121−231) variants and their solubility in the periplasm. The five variants with the lowest stabilities, i.e., Asp178Asn, Met129Val/Asp178Asn, Thr183Ala, Phe198Ser, and Glu217Arg, are exactly those which accumulated in periplasmic indusion bodies, while all other variants with wild type-like stabilities were obtained as soluble proteins (Figure 3, Table 1). This observation is in line with earlier reports that protein stability is correlated with the yield of functionally expressed protein in the periplasm of *E. coli* (*51*). However, we do not expect that similar misfolding events would necessarily occur with the corresponding PrP^{C} variants in patients with inherited TSEs, because inclusion body formation is mostly a consequence of unspecific aggregation and thus not related to specific PrP^{Sc} aggregates with an ordered array of protein subunits of identical fold. In addition, folding of the insoluble variants is completely reversible in our experiments, and the periplasm of *E. coli* provides a biological environment rather different from the one the posttranslationally modified prion protein is exposed to within eukaryotes.

A detailed analysis of the location of the amino acid replacements related to human TSE in the refined NMR structure of *m*PrP(121−231) has recently been published (*27*) (Figure 2). The isosteric replacement of aspartate 178 to asparagine in the variants Asp178Asn and Asp178Asn/Met129Val affects a solvent-accessible salt bridge (Arg164-H^{η}/O^{δ}-Asp178) and a hydrogen bond (Tyr128-H^{η}/O^{δ}-Asp178) which connect both β-strands with helix 2 (*27*). This exchange destabilizes the protein by 7−8 kJ mol^{-1} independent of the human Met/Val polymorphism at position 129. Although hydrogen bonds located at the molecular surface tend to contribute little to protein stability (0−2 kJ mol^{-1}) (*52*, *53*) and the modified interactions of the asparagine side chain with the hydrogen bond partners are difficult to assess, the exchange Asp178Asn might further destabilize the proteins by a structural rearrangement between the β-sheet and helix 2. A slightly stronger destabilization was obtained for the exchange of the partially buried Gln217 by Arg which removes a buried hydrogen bond between helix 3 and an adjacent well-defined loop (Gln217-$H^{\epsilon}/\psi O'$-Ala133) (*27*). While buried hydrogen bonds contribute about 4−8 kJ mol^{-1} to stability (*52*−*54*), introduction of the bulkier and charged arginine side chain may create steric strains and unfavorable interactions with its hydrophobic environment in the folded state. The variant Thr183Ala is strongly destabilized by about 19 kJ mol^{-1} due to the loss of two buried hydrogen bonds of the threonine side chain to residues in the hydrophobic core (Tyr162-H^{N}/O^{γ}-Thr183, Thr183-OH^{γ}/O'-Cys179) (*27*) and the loss of van der Waal's interactions of the deleted side chain atoms with the protein. The exchange of Phe198 for Ser creates a cavity in the interior of the molecule and lowers the van der Waal's interaction and the buried hydrophobic surface area due to the loss of the phenylalanine, while a polar side chain is introduced into the hydrophobic core.

The valine side chains at positions 180 and 210 both contribute to the hydrophobic protein core, but their replacement by the bulkier isoleucine side chains in the variants Val180Ile and Val210Ile barely affects the stability of *m*PrP-(121−231). The unfavorable packing interactions caused by the isoleucine side chain seem to be fully compensated by the introduction of a single methylene group buried in the folded state, for which a stabilization of 6 ± 2 kJ mol^{-1} due to van der Waal's contacts and hydrophobic effects is expected (*55*−*58*). Surprisingly, the substitution of Glu200 by Lys at the N-terminus of helix 3 does not alter the thermodynamic stability, although an unfavorable interaction of the positively charged lysine side chain with the helix dipole seems possible (*53*, *59*). The exchange of the solvent-exposed Arg208 for His in helix 3 is probably destabilizing due to the low α-helix propensity of histidine, since its aromatic β-substitution lowers the side chain entropy upon helix formation (*60*−*62*).

The replacement related to the nonpathogenic Met/Val polymorphism at position 129 in humans has no effect on the thermodynamic stability of *m*PrP(121−231). This polymorphism at the solvent-exposed residue 129 in the first β-strand of PrP^{C} determines the disease phenotype linked to the Asp178Asn substitution in such a way that the Met129/Asn178 allele segregates with FFI whereas the Val129/Asn178 allele segregates with familial CJD (*35*). The higher β-sheet propensity of Val compared to Met (*63*, *64*) located in the first β-strand of *m*PrP(121−231) is thus not sufficient to stabilize *m*PrP(121−231), possibly due to the exposure of residue 129 to the solvent.

A polymorphism in the murine PrP gene (*Prn-p*) at positions 108 and 189 (equivalent to positions 109 and 190

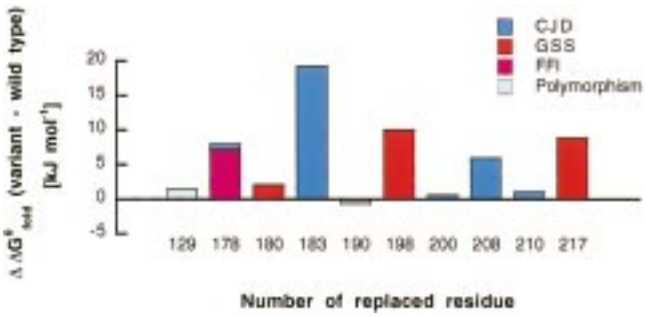

FIGURE 6: Thermodynamic stabilities of *m*PrP(121−231) variants relative to *m*PrP(121−231) wild type. $\Delta\Delta G°_{fold}$ (variant − wild type) is shown for each point mutation site by bars which are colored according to the related disease phenotype (same color code as in Figure 1). Positive $\Delta\Delta G°_{fold}$ values indicate that the variant is less stable than the wild type protein.

in recombinant *m*PrP) has been genetically linked to the scrapie incubation time in mice and thus to the susceptibility to scrapie (*36*, *65*, *66*). The short incubation time *Prn-p*^{a} mice encode leucine and threonine at positions 108 and 189, respectively, whereas phenylalanine and valine are present in long incubation time *Prn-p*^{b} mice (*36*, *67*). Amino acid residue 190 is located in helix 2 of *m*PrP(121−231). The isosteric substitution of theronine by valine at this position has no influence on protein stability, presumably since both β-branched side chains have a similar, very low α-helix propensity (*68*). No significant influence on protein stability is also expected for the replacement Leu109Phe, since residue 109 is located in the unstructured N-terminal segment of *m*PrP^C. However, if the criterion of PrP^C stability is a major determinant which governs the onset of the disease, the amino acid substitution at position 190 should significantly have increased the thermodynamic stability of PrP^C.

The stabilities of all *m*PrP(121−231) variants obtained from urea-induced equilibrium transitions do not correlate with any particular prion disease phenotype as presented in Figure 6. GSS and familiar CJD are both linked to amino acid exchanges with either a destabilizing or no effect on the thermodynamic stability of *m*PrP(121−231). This observation indicates that the stability of PrP^C is not the general determinant and not the only factor that triggers the spontaneous generation of PrP^{Sc} in inherited TSEs. The PrP^C → PrP^{Sc} conversion following a yet unknown molecular mechanism may thus be facilitated by other physical properties of the variants such as the following: (i) an increased stability of PrP^{Sc}; (ii) an increased fraction of alternative conformations that are in equilibrium with PrP^C and may act as precursors of oligomeric PrP^{Sc} (*48*, *69*, *70*); (iii) different folding kinetics of PrP^C with accumulation of PrP^{Sc}-like kinetic folding intermediates; (iv) an altered interaction with other yet unknown cellular cofactors, chaperones, or proteins, such as with protein "X", a presumed host factor that may be required for formation of PrP^{Sc} (*71*) or the presumed natural PrP^C ligand L$_{PrP}$ (*29*). It is possible that several of these factors act in combination in the process of scrapie formation.

For several reasons, one can assume that the amino acid substitutions in *m*PrP(121−231) influence the stability of the full-length prion protein, *m*PrP(23−231), in a similar manner. The structure of the C-terminal domain, *m*PrP(121−231), is retained in the murine full-length prion protein, *m*PrP(23−231), whose additional N-terminal segment of 98 amino acid residues is highly flexible in solution (*11*). Both *m*PrP(121−231) and *m*PrP(23−231) exhibit cooperative and completely reversible urea-induced unfolding transitions at pH 7.0 with identical midpoint concentrations of the denaturant. The lowered cooperativity causing the slight destabilization of full-length *m*PrP may result from contacts between residues from the N- and C-terminal parts of the protein in the unfolded state which would reduce the difference in the solvent-accessible surface area between the folded and unfolded states (*72*). A lower stability of *m*PrP(23−231) may principally also be explained by interactions of segment 23−120 with the C-terminal domain in native PrP^C as proposed from the NMR structure of hamster PrP (*10*, *28*), causing a loss of conformational entropy of the N-terminal segment (*73*, *74*). However, such an interaction could not be detected in full-length *m*PrP(23−231) (*11*).

One might argue that the recombinant *m*PrP proteins used in our studies lack the two N-glycosylation sites and the GPI membrane anchor, but there is biochemical evidence that both posttranslational modifications are not essential for the process of scrapie formation. Unglycosylated PrP^C molecules, in which the N-glycosylation was blocked either by inhibitors or by mutagenesis, were converted into PrP^{Sc} (*75*), and deletion of the C-terminal pro-peptide for addition of the GPI anchor was found to diminish but not to abolish PrP^{Sc} synthesis in scrapie-infected neuroblastoma cells (*76*).

For several murine PrP proteins carrying different mutations associated with inherited TSEs, the production in Chinese hamster ovary cells has been reported (*77*−*81*). The *m*PrP variants Pro102Leu, Asp178Asn/Met129, Thr183Ala, and Glu200Lys (numbering according to human PrP) and a protein with an insertion of six additional octapeptide repeats displayed a number of biochemical hallmarks characteristic of PrP^{Sc} such as detergent insolubility, protease resistance, aberrant membrane attachment, and hydrophobicity. The amino acid exchange Thr183Ala blocked the delivery of the protein to the cell surface probably due to inactivation of the N-glycosylation site at Asn181, but the characterization of the other variants showed that defects in biosynthetic trafficking are not a general feature of pathologic mutations in PrP (*81*). Although these mutant *m*PrPs are distinguished from each other by several biochemical features such as the size of their protease-resistant cores or the glycosylation patterns (*78*), the thermodynamic stabilities of the analogous variants of *m*PrP(121−231) measured in this study do not correlate with these properties. An exception is the Met/Val polymorphism at postion 129 which has no influence on protein stability (Table 1) and also does not induce PrP^{Sc}-like aggregates in cultured cells (*78*). In other studies, the expression of human PrP genes harboring the Asp178Asn mutation with Met129/Val129 (*82*) and the Gln217Arg mutation (*83*) in human neuroblastoma cells has been described. These results suggested an instability of the proteins with the Asp178Asn exchange in vivo (*82*) and temperature-dependent protein misfolding in the case of the Gln217Arg variant (*83*).

The investigation of the allelic origin of the protease-resistant PrP^{Sc} oligomer isolated from patients with inherited mutations in the PrP gene yielded different results for the individual mutations. Whereas in the case of the five different PrP mutations at positions 102, 178, 198, 200, and 217 linked

with GSS, and familial CJD, only the mutant PrP^C forms protease-resistant PrP^{Sc} (*84*−*88*), the mutation at position 210 (*89*) and also the insertion of five or six additional octapeptide repeats (*88*), all linked with familial CJD, led to heterooligomeric, protease-resistant PrP^{Sc} deposits in the brain of the patients. Altogether, these in vivo data cannot be rationalized on the basis of the thermodynamic stabilities of *m*PrP(121−231) variants measured in vitro. For example, the observation that the amino acid replacement Val210Ile has no effect on the intrinsic stability of *m*PrP(121−231) suggests similar tendencies of wild type and mutant PrP^C to be converted into PrP^{Sc} (*89*), but in case of the exchange Glu200Lys, which does not affect the stability either, only the mutant PrP is converted into the protease-resistant form (*87*). Thus, the homo- or heterooligomeric association state of PrP^{Sc} in inherited TSEs may instead be determined by the interactions in a supposed PrP^C/PrP^{Sc} heterodimer (*5*) or by the ability of monomeric PrP^{Sc} precursors to become incorporated into a regular array of subunits in the PrP^{Sc} oligomer (*70*).

In conclusion, our thermodynamic stability measurements show that the specific point mutations associated with inherited human prion diseases are unlikely to be a determinant for the $PrP^C \rightarrow PrP^{Sc}$ conversion exclusively due to a lowered thermodynamic stability of PrP^C. Consequently, other mechanisms that could lead to the spontaneous development of prions in inherited human TSEs also have to be considered. This view is supported by the findings that mice overexpressing a murine PrP transgene with the human GSS mutation Pro102Leu, which is assumed to be non-destabilizing for PrP^C, spontaneously develop a lethal and infectious scrapie-like disease (*90*, *91*), whereas the non-destabilizing Glu200Lys mutation did not cause a TSE-like illness (*92*).

ACKNOWLEDGMENT

We are very grateful to J. Hennecke for helpful advice. We thank M. Billeter, G. Cereghetti, E. Flechsig, M. Huber-Wunderlich, S. Hornemann, E. Leclerc-L'Hostis, R. Riek, P. Sebbel, G. Wildegger, G. Wider, and K. Wüthrich for fruitful discussions, G. Frank for Edman sequencing, and P. James for performing mass spectrometry.

REFERENCES

1. Weissmann, C., Fischer, M., Raeber, A., Büeler, H., Sailer, A., Shmerling, D., Rülicke, T., Brandner, S., and Aguzzi, A. (1996) *Cold Spring Harbor Symp. Quant. Biol. 61*, 511−522.
2. Prusiner, S. B. (1997) *Science 278*, 245−251.
3. Griffith, J. S. (1967) *Nature 215*, 1043−1044.
4. Gajdusek, D. C. (1988) *J. Neuroimmunol. 20*, 95−110.
5. Prusiner, S. B. (1991) *Science 252*, 1515−1522.
6. Basler, K., Oesch, B., Scott, M., Westaway, D., Wälchli, M., Groth, D. F., McKinley, M. P., Prusiner, S. B., and Weissmann, C. (1986) *Cell 46*, 417−428.
7. Stahl, N., and Prusiner, S. B. (1991) *FASEB J. 5*, 2799−2807.
8. Prusiner, S. B. (1992) *Biochemistry 31*, 12277−12288.
9. Pan, K.-M., Baldwin, M., Nguyen, J., Gasset, M., Serban, A., Groth, D., Mehlhorn, I., Huang, Z., Fletterick, R. J., Cohen, F. E., and Prusiner, S. B. (1993) *Proc. Natl. Acad. Sci. U.S.A. 90*, 10962−10966.
10. Donne, D. G., Viles, J. H., Groth, D., Mehlhorn, I., James, T. L., Cohen, F. E., Prusiner, S. B., Wright, P. E., and Dyson, H. J. (1997) *Proc. Natl. Acad. Sci. U.S.A. 94*, 13452−13457.
11. Riek, R., Hornemann, S., Wider, G., Glockshuber, R., and Wüthrich, K. (1997) *FEBS Lett. 413*, 282−288.
12. Caughey, B. W., Dong, A., Bhat, K. S., Ernst, D., Hayes, S. F., and Caughey, W. S. (1991) *Biochemistry 30*, 7672−7680.
13. Safar, J., Roller, P. R., Gajdusek, D. C., and Gibbs, C. J. (1993) *J. Biol. Chem. 268*, 20276−20284.
14. Oesch, B., Westaway, D., Wälchli, M., McKinley, M. P., Kent, S. B. H., Aebersld, R., Barry, R. A., Tempst, P., Teplow, D. B., Hood, L. E., Prusiner, S. B., and Weissmann, C. (1985) *Cell 40*, 735−746.
15. Meyer, R. K., McKinley, M. P., Bowman, K. A., Braunfeld, M. B., Barry, R. A., and Prusiner, S. B. (1986) *Proc. Natl. Acad. Sci. U.S.A. 833*, 2310−2314.
16. McKinley, M. P., Meyer, R. K., Kenaga, L., Rahbar, F., Cotter, R., Serban, A., and Prusiner, S. B. (1991) *J. Virol. 65*, 1340−1351.
17. Chesebro, B. (1998) *Science 279*, 42−43.
18. Büeler, H., Aguzzi, A., Sailer, A., Greiner, R., Autenried, P., Aguet, M., and Weissmann, C. (1993) *Cell 73*, 1339−1347.
19. Fischer, M., Rulicke, T., Raeber, A., Sailer, A., Moser, M., Oesch, B., Brandner, S., Aguzzi, A., and Weissmann, C. (1996) *EMBO J. 15*, 1255−1264.
20. Schätzl, H. M., Da Costa, M., Taylor, L., Cohen, F. E., and Prusiner, S. B. (1995) *J. Mol. Biol. 245*, 362−374.
21. Billeter, M., Riek, R., Wider, G., Hornemann, S., Glockshuber, R., and Wüthrich, K. (1997) *Proc. Natl. Acad. Sci. U.S.A. 94*, 7281−7285.
22. Stahl, N., Borchelt, D. R., Hsiao, K., and Prusiner, S. B. (1987) *Cell 51*, 229−240.
23. Stahl, N., Borchelt, D. R., and Prusiner, S. B. (1990) *Biochemistry 29*, 5405−5412.
24. Endo, T., Groth, D., Prusiner, S. B., and Kobata, A. (1989) *Biochemistry 28*, 8380−8388.
25. Turk, E., Teplow, D. B., Hood, L. E., and Prusiner, S. B. (1988) *Eur. J. Biochem. 176*, 21−30.
26. Riek, R., Hornemann, S., Wider, G., Billeter, M., Glockshuber, R., and Wüthrich, K. (1996) *Nature 382*, 180−182.
27. Riek, R., Wider, G., Billeter, M., Hornemann, S., Glockshuber, R., and Wüthrich, K. (1998) *Proc. Natl. Acad. Sci. U.S.A. 95*, 11667−11672.
28. James, T. L., Liu, H., Ulyanov, N. B., Farr-Jones, S., Zhang, H., Donne, D. G., Kaneko, K., Groth, D., Mehlhorn, I., Prusiner, S. B., and Cohen, F. E. (1997) *Proc. Natl. Acad. Sci. U.S.A. 94*, 10086−10091.
29. Shmerling, D., Hegyi, I., Fischer, M., Blättler, T., Brandner, S., Götz, J., Rülicke, T., Flechsig, E., Cozzio, A., von Mering, C., Hangartner, C., Aguzzi, A., and Weissmann, C. (1998) *Cell 93*, 203−214.
30. Goldfarb, L. G., Brown, P., Cervenakova, L., and Gajdusek, D. C. (1994) *Philos. Trans. R. Soc. London B 343*, 379−384.
31. Prusiner, S. B. (1996) in *Prions, Prions, Prions* (Prusiner, S. B., Ed.) pp 1−18, Springer-Verlag, Berlin, Heidelberg, and New York.
32. Cohen, F. E., Pan, K.-M., Huang, Z., Baldwin, M., Fletterick, R. J., and Prusiner, S. B. (1994) *Science 264*, 530−531.
33. Huang, Z., Gabriel, J. M., Baldwin, M. A., Fletterick, R. J., Prusiner, S. B., and Cohen, F. E. (1994) *Proc. Natl. Acad. Sci. U.S.A. 91*, 7139−7143.
34. Huang, Z., Prusiner, S. B., and Cohen, F. E. (1995) *Folding Des. 1*, 13−19.
35. Goldfarb, L. G., Petersen, R. B., Tabaton, M., Brown, P., LeBlanc, A. C., Montagna, P., Cortelli, P., Julien, J., Vital, C., Pendelbury, W. W., Haltia, M., Wills, P. R., Hauw, J. J., McKeever, P. E., Monari, L., Schrank, B., Swergold, G. D., Autilio-Gambetti, L., Gajdusek, D. C., Lugaresi, E., and Gambetti, P. (1992) *Science 258*, 806−808.
36. Westaway, D., Goodman, P. A., McKinley, M. P., Carlson, G. A., and Prusiner, S. B. (1987) *Cell 51*, 651−662.
37. Hornemann, S., and Glockshuber, R. (1996) J. Mol. Biol. 261, 614−619.
38. Kunkel, T. A. (1985) *Proc. Natl. Acad. Sci. U.S.A. 82*, 488−492.
39. Kunkel, T. A., Roberts, J. D., and Zabour, R. A. (1987) *Methods Enzymol. 154*, 367−382.

40. Vieira, J., and Messing, J. (1987) *Methods Enzymol. 153*, 3−11.
41. Hornemann, S., Korth, C., Oesch, B., Riek, R., Wider, G., Wüthrich, K., and Glockshuber, R. (1997) *FEBS Lett. 413*, 277−281.
42. Strobl, S., Mühlhahn, P., Bernstein, R., Wiltscheck, R., Maskos, K., Wunderlich, M., Huber, R., Glockshuber, R., and Holak, T. (1995) *Biochemistry 34*, 8281−8293.
43. Studier, F. W., and Moffatt, B. A. (1986) *J. Mol. Biol. 189*, 113−130.
44. Ellman, G. L. (1959) *Arch. Biochem. Biophys. 82*, 70−77.
45. Gill, S. C., and von Hippel, P. H. (1989) *Anal. Biochem. 182*, 319−326.
46. Warren, J. R., and Gordon, J. A. (1966) *J. Phys. Chem. 67*, 1524−1527.
47. Santoro, M. M., and Bolen, D. W. (1988) *Biochemistry 27*, 8063−8068.
48. Hornemann, S., and Glockshuber, R. (1998) *Proc. Natl. Acad. Sci. U.S.A. 95*, 6010−6014.
49. Pace, C. N. (1986) *Methods Enzymol. 131*, 266−280.
50. Swietnicki, W., Petersen, R. B., Gambetti, P., and Surewicz, W. K. (1998) *J. Biol. Chem. 273*, 31048−31052.
51. Frisch, C., Kolmar, H., Schmidt, A., Kleemann, G., Reinhardt, A., Pohl, E., Usòn, I., Schneider, T. R., and Fritz, H.-J. (1996) *Folding Des. 1*, 431−440.
52. Serrano, L., Kellis, J. T. J., Cann, P., Matouschek, A., and Fersht, A. R. (1992) *J. Mol. Biol. 224*, 783−804.
53. Fersht, A. R., and Serrano, L. (1993) *Curr. Opin. Struct. Biol. 3*, 75−83.
54. Shirley, B. A., Stanssens, P., Hahn, U., and Pace, C. N. (1992) *Biochemistry 31*, 725−732.
55. Kellis, J. T., Nyberg, K., Sali, D., and Fersht, A. R. (1988) *Nature 333*, 784−786.
56. Shortle, D., Stites, W. E., and Meeker, A. K. (1990) *Biochemistry 29*, 8033−8041.
57. Erikksson, E., Baase, W. A., Zhanf, X.-J., Heinz, D. W., Blaber, M., Baldwin, E. P., and Matthews, B. W. (1992) *Science 255*, 178−183.
58. Pace, C. N. (1992) *J. Mol. Biol. 226*, 29−35.
59. Hol, W. G. J. (1985) *Prog. Biophys. Mol. Biol. 45*, 149−195.
60. O'Neil, K. T., and DeGrado, W. F. (1990) *Science 250*, 646−651.
61. Horovitz, A., Matthews, J. M., and Fersht, A. R. (1992) *J. Mol. Biol. 227*, 560−568.
62. Blaber, M., Zhang, X.-J., and Matthews, B. W. (1993) *Science 260*, 1637−1640.
63. Kim, C. A., and Berg, J. M. (1993) *Nature 362*, 267−270.
64. Smith, C. K., Withka, J. M., and Regan, L. (1994) *Biochemistry 33*, 5510−5517.
65. Carlson, G. A., Kingsbury, D. T., Goodman, P. A., Coleman, S., Marshall, S. T., DeArmond, S. J., Westaway, D., and Prusiner, S. B. (1986) *Cell 46*, 503−511.
66. Carlson, C. A., Westaway, D., DeArmond, S. J., Peterson-Torchia, M., and Prusiner, S. B. (1989) *Proc. Natl. Acad. Sci. U.S.A. 86*, 7475−7479.
67. Moore, R. C., Hope, J., McBride, P. A., McConnell, I., Selfridge, J., Melton, D. W., and Manson, J. C. (1998) *Nat. Genet. 18*, 118−125.
68. Chakrabartty, A., and Baldwin, R. L. (1994) *Q. Rev. Biophys. 26*, 141−176.
69. Swietnicki, W., Petersen, R., Gambetti, P., and Surewicz, W. K. (1997) *J. Biol. Chem. 272*, 27517−27520.
70. Jarrett, J. T., and Lansbury, P. T., Jr. (1993) *Cell 73*, 1055−1058.
71. Telling, G. C., Scott, M., Mastrianni, J., Gabizon, R., Torhia, M., Cohen, F. E., DeArmond, S. J., and Prusiner, S. B. (1993) *Cell 83*, 79−90.
72. Myers, J. K., Pace, C. N., and Scholtz, J. M. (1995) *Protein Sci. 4*, 2138−2148.
73. Ladurner, A. G., and Fersht, A. R. (1997) *J. Mol. Biol. 273*, 330−337.
74. Nagi, A. D., and Regan, L. (1997) *Folding Design 2*, 67−75.
75. Taraboulos, A., Rogers, M., Borchelt, D. R., McKinley, M. P., Scott, M., Serban, D., and Prusiner, S. B. (1990) *Proc. Natl. Acad. Sci. U.S.A. 87*, 8262−8266.
76. Rogers, M., Yehiely, F., Scott, M., and Prusiner, S. B. (1993) *Proc. Natl. Acad. Sci. U.S.A. 90*, 3182−3186.
77. Lehmann, S., and Harris, D. A. (1995) *J. Biol. Chem. 270*, 24589−24597.
78. Lehmann, S., and Harris, D. A. (1996) *J. Biol. Chem. 271*, 1633−1637.
79. Lehmann, S., and Harris, D. A. (1996) *Proc. Natl. Acad. Sci. U.S.A. 93*, 5610−5614.
80. Daude, N., Lehmann, S., and Harris, D. A. (1997) *J. Biol. Chem. 272*, 11604−11612.
81. Lehmann, S., and Harris, D. A. (1997) *J. Biol. Chem. 272*, 21479−21487.
82. Petersen, R. B., Parchi, P., Richardson, S. L., Urig, C. B., and Gambetti, P. (1996) *J. Biol. Chem. 271*, 12661−12668.
83. Singh, N., Zanusso, G., Chen, S. G., Fujioka, H., Richardson, S., Gambetti, P., and Petersen, R. B. (1997) *J. Biol. Chem. 272*, 28461−28470.
84. Kitamoto, T., Yamaguchi, K., Dohura, K., and Tateishi, J. (1991) *Neurology 41*, 306−310.
85. Tagliavini, F., Prelli, F., Porro, M., Rossi, G., Giaccone, G., Farlow, M. R., Dlouhy, S. R., Ghetti, B., Bugiani, O., and Frangione, B. (1994) *Cell 79*, 695−703.
86. Barbanti, P., Fabbrini, G., Salvatore, M., Petraroli, R., Cardone, F., Maras, B., Equestre, M., Macchi, G., Lenzi, G. L., and Pocchiari, M. (1996) *Neurology 47*, 734−741.
87. Gabizon, R., Telling, G., Meiner, Z., Halimi, M., Kahana, I., and Prusiner, S. B. (1996) *Nat. Med. 2*, 59−64.
88. Chen, S. G., Parchi, P., Brown, P., Capellari, S., Zou, W., Cochran, E. J., Vnencak-Jones, C. L., Julien, J., Vital, C., Mikol, J., Lugaresi, E., Autilio-Gambetti, L., and Gambetti, P. (1997) *Nat. Med. 3*, 1009−1015.
89. Silvestrini, M. C., Cardone, F., Maras, B., Pucci, P., Barra, D., Brunori, M., and Pocchiari, M. (1997) *Nat. Med. 3*, 521−525.
90. Hsiao, K. K., Scott, M., Foster, D., Groth, D. F., DeArmond, S. J., and Prusiner, S. B. (1990) *Science 250*, 1587−1590.
91. Hsiao, K. K., Groth, D., Scott, M., Yang, S. L., Serban, H., Rapp, D., Foster, D., Torchia, M., DeArmond, S. J., and Prusiner, S. B. (1994) *Proc. Natl. Acad. Sci. U.S.A. 91*, 9126−9130.
92. Telling, G. C., Haga, T., Torchia, M., Tremblay, P., DeArmond, S. J., and Prusiner, S. B. (1996) *Genes Dev. 10*, 1736−1750.
93. Koradi, R., Billeter, M., and Wüthrich, K. (1996) *J. Mol. Graphics 14*, 52−55.

BI982714G